Proceedings of IPACK2007
ASME InterPACK '07
July 8-12, 2007, Vancouver, British Columbia, CANADA

IPACK2007-33124

ANALYTICAL SOLUTION OF WHISPERING-GALLERY MODES

Haiyong Quan
Dept. of Mechanical and Aerospace Engineering
Rutgers, The State University of New Jersey
98 Brett Road, Piscataway, NJ 08854

Zhixiong Guo
Dept. of Mechanical and Aerospace Engineering
Rutgers, The State University of New Jersey
98 Brett Road, Piscataway, NJ 08854

ABSTRACT

Advances in MEMS/NEMS techniques have enabled high-Q whispering-gallery modes in integrated microcavities. Potential applications of optical microcavities include quantum informatics, novel micro/nano sources, dynamic filters, and micro/nanosensors. It is important to understand the intrinsic resonant modes of a cavity. In this report, we will analyze whispering-gallery modes in resonators of planar structure which is common in MEMS devices. The wave equation is solved by using the method of separation of variables with appropriate boundary conditions. Analytical formulations are established. The resonance frequencies as well as the electric field distributions in exemplary resonators are presented for a variety of whispering-gallery modes.

INTRODUCTION

The concept of whispering-gallery (WG) modes was first introduced by Rayleigh to elucidate why sound waves travel more efficiently along the inside wall of a circularly-shaped structure.[1] When WG modes occur in optical wavelength range, the resonator can be shrunk to the micrometer level. In 1961 Garrett *et al*.[2] at Bell Labs reported the observation of optical WG modes in spherical CaF_2 particles doped with Sm^{++} which were illuminated by a high-pressure xenon flashtube. In 1987 Braginsky and Ilchenko[3] generated high-Q WG modes in fused-silica microspheres. In recent years ultrahigh-Q ($>10^9$) has been reported,[4] and optical microcavities have received increasing attention due to their high potentials in quantum informatics,[5] novel micro/nano sources, dynamic filters, and micro/nanosensors.[6]

The extraordinary demand for integrated techniques and miniaturization presents a major challenge to the technical community. Nowadays it is feasible to consider WG modes in fine and uniform devices having physical dimensions at micro- and nanometer scales. For example, Zhang *et al*.[7] built an InGaAsP micro-laser with a ring cavity of 4.5μm in diameter and a curing waveguide of 0.4μm in width. Krioukov *et al*.[8] considered integrated microcavities for enhanced evanescent-wave spectroscopy. The waveguide and semiconductor nanofabrication techniques enable mass production of compactly integrated and robust lab-on-a-chip WG mode devices. Most such devices have planar structures.

Analytical tools are in great demand for guiding the design of Opto-MEMS/NEMS devices. Optical WG modes are rigorously governed by Maxwell electromagnetic (EM) theory. The geometric optics method[9] can only be used for roughly estimating some simple WG modes. Numerical approaches[10] are approximate although they take advantages in complex systems and can be utilized to investigate such as the gap effects.[11] Analytical methods give exact solutions to a physical problem.

The objective of this report is to analyze WG modes of planar resonators. In EM analyses, the scattering of a plane wave is usually adopted and the wave equations are solved.[12] In this manuscript the electric wave equation is solved via the method of separation of variables. Appropriate boundary conditions are set up to close the physical solutions. The formulations are derived. The WG mode electric-field distributions as well as the resonant frequencies of two exemplary cavities are obtained and presented

NOMENCLATURE

- a = radius
- E = electric field
- l = radial mode number
- m = polar mode number
- n = azimuthal mode number; refractive index
- r = radial direction
- k = wave number
- λ = wavelength
- θ = azimuthal angle

ANALYSES

Figure 1 schematically shows a WG mode in a sphere. Light is trapped in circular orbits along the equatorial plane within the surface of the structure and can be thought to propagate along zigzag paths. WG modes in the spherical coordinates are characterized by three mode numbers: l, n and m, which are the radial, azimuthal and polar mode numbers, respectively. The mode number l is equal to the number of field maxima in the radial direction (r) of the sphere. The value of $2n$ indicates the number of field maxima in the azimuthal direction (θ) in an equatorial plane, and the value of ($n-m+1$) is equal to the number of field maxima in the polar direction (φ) around the equator.

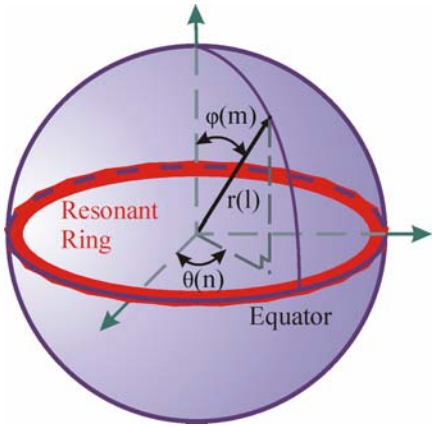

Figure 1. Schematic of a WG mode in a sphere.

In planar structures, only l and n modes are needed for describing WG modes. Consider a harmonic in-plane TM wave, the E-field has only the z-component, E_z; and the scalar Helmholtz's equation in a disk coordinate is[12]

$$\frac{\partial^2 E_z}{\partial r^2}+\frac{1}{r}\frac{\partial E_z}{\partial r}+\frac{1}{r^2}\frac{\partial^2 E_z}{\partial \theta^2}+k^2 E_z=0 \qquad (1)$$

where the wave number $k=\omega\sqrt{\mu\varepsilon}$. ε and μ are the permittivity and permeability, respectively.

To solve the above equation we assume a separation in the form

$$E_z = R(r)\Theta(\theta) \qquad (2)$$

and introduce a separation variable *n*. Then Eq. (1) is separated into two ordinary differential equations:

$$\Theta''+n^2\Theta=0 \qquad (3a)$$

$$R''+\frac{1}{r}R'+(k^2-\frac{n^2}{r^2})R=0 \qquad (3b)$$

By choosing a proper reference line from which θ is measured, the solutions of Θ can be formulized as

$$\Theta_n(\theta)=A_n\cos(n\theta),\ n=1,2,3... \qquad (4)$$

Thus, the eigenvalues of the separation variable *n* are actually the feasible azimuthal modes.

There are two solutions for Eq. (3b). For EM waves inside the resonator, i.e., if $r<a$, where a is the physical radius of the disk resonator, we have

$$R_i(r)=C_n J_n(k_1 r) \qquad (5)$$

For EM waves outside the resonator, i.e., if $r>a$, the solution for Eq. (3b) becomes the real part of

$$R_o(r)=D_n H_n(k_2 r) \qquad (6)$$

where the Hankel function is defined as $H_n(x)=J_n(x)\pm iY_n(x)$. k_1 and k_2 denote the wave numbers in and out the resonator, respectively.

By applying the continuity boundary condition

$$R_i(a)=R_o(a) \qquad (7)$$

we can correlate D_n with C_n and get a solution:

$$R_o(r)=C_n J_n(k_1 a)\frac{J_n(k_2 a)J_n(k_2 r)+Y_n(k_2 a)Y_n(k_2 r)}{J_n^2(k_2 a)+Y_n^2(k_2 a)} \qquad (8)$$

The general eigenfunctions of E_z, which can be interpreted as the possible spatial WG modes, are then the products of the solutions for Θ and R as follows:

for $r \le a$,

$$E_{zn}(r,\theta)=G_n J_n(k_1 r)\cos(n\theta) \qquad (9)$$

for $r > a$,

$$E_{zn}(r,\theta)=G_n J_n(k_1 a)\frac{J_n(k_2 a)J_n(k_2 r)+Y_n(k_2 a)Y_n(k_2 r)}{J_n^2(k_2 a)+Y_n^2(k_2 a)}\cos(n\theta) \qquad (10)$$

with n = 1, 2, 3 …

Consider the continuity condition of the first derivative of E_z with respect to r at $r=a$

$$\left.\frac{dR_i}{dr}\right|_{r=a}=\left.\frac{dR_o}{dr}\right|_{r=a} \qquad (11)$$

It follows that

$$\frac{n_1}{n_2}\frac{J_n'(k_1 a)}{J_n(k_1 a)}=\frac{J_n(k_2 a)J_n'(k_2 a)+Y_n(k_2 a)Y_n'(k_2 a)}{J_n^2(k_2 a)+Y_n^2(k_2 a)} \qquad (12)$$

Where n_1 and n_2 are the refractive indices of the materials in and out the resonator, respectively. This boundary condition is then utilized for finding the possible resonance wavelengths for a WG mode *n* via iteration and bisection methods.

Now we need one more condition to determine where the radial component of the E-field peaks and valleys for the obtained resonance wavelengths. Since WG modes are confined inside a resonator, we only need to calculate

$$\frac{\partial E_z}{\partial r}=0 \ \text{ for } r<a \qquad (13)$$

From $J_n'(k_1 r)=0$, we obtain the equation below for finding the radial positions of peaks and valleys:

$$k_1 r J_{n-1}(k_1 r)-nJ_n(k_1 r)=0 \qquad (14)$$

The number of peaks and valleys accounts for the l mode number, and the wavelength λ_{ln} is the resonance wavelength for a WG mode (l, n).

Table 1. Resonance wavelengths of a 2μm-diameter resonator at various WG modes.

Mode n	Resonance λ (nm)	FSR (nm)
1	5629.1504	
		2053.7598
2	3575.3906	
		926.9531
3	2648.4375	
		548.999
4	2099.4385	
		353.2959
5	1746.1426	
		248.6634
6	1497.4792	
		184.5153
7	1312.9639	
		142.4164
8	1170.5475	
		113.2828
9	1057.2647	
		92.3737
10	964.891	
		76.8642
11	888.0268	
		65.032
12	822.9948	
		55.7975
13	767.1973	
		48.4423
14	718.755	
		42.4827
15	676.2723	
		37.5815
16	638.6908	
		33.4985
17	605.1923	
		30.0585
18	575.1338	
		27.1316
19	548.0022	
		24.6191
20	523.3831	
		22.4456
21	500.9375	
		20.5518
22	480.3857	

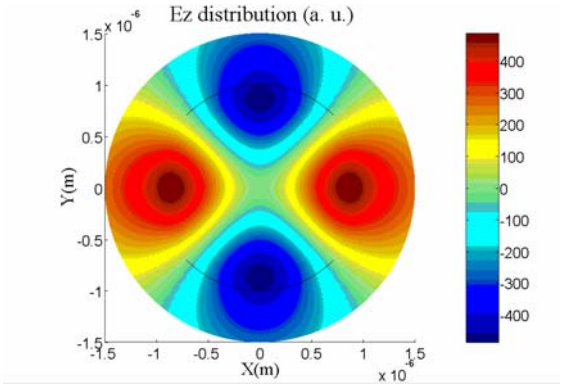

$n = 2$

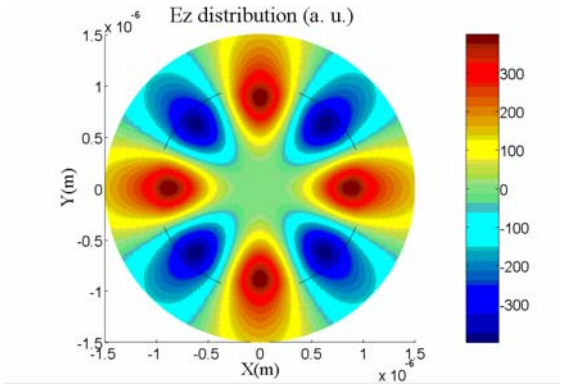

$n = 4$

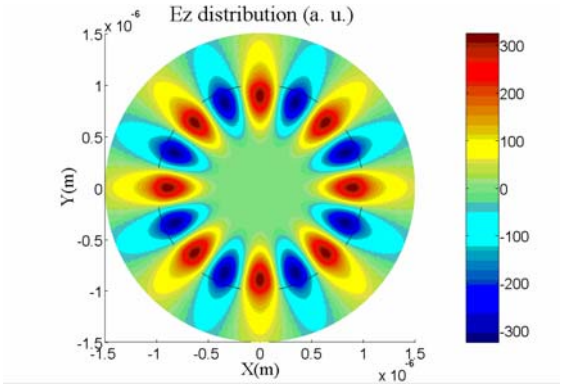

$n = 8$

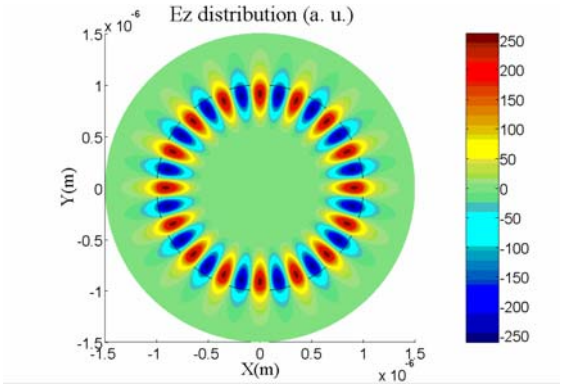

$n = 16$

Figure 2. E-field distributions for different azimuthal mode numbers with $l = 1$.

RESULTS AND DISCUSSION

Let us consider two exemplary disk resonators made of silicon nitride and exposed to the ambient air. The refractive index is 2.01 for Si_3N_4 and 1.0 for air. Table 1 lists the resonance wavelengths of a 2μm-diameter resonator for various azimuthal modes at the same radial mode l =1. The resonance wavelength decreases with the increase of the azimuthal mode number. The free spectrum range (FSR) also decreases with increasing mode number. Thus, the resonance spectrum of a resonator is not uniformly distributed.

Figure 2 shows the E-field distributions for four different azimuthal mode numbers at a radial mode l =1. The dark circles in the maps mark the physical boundary of the resonator (a = 1μm). The larger is the azimuthal mode number, the narrower is the confined mode region.

Further inspection of the radial profile of normalized E_z as shown in Fig. 3, it is confirmed that with increasing azimuthal mode number, more energy will be confined in a very thin layer inside the resonator surface and less energy will leak out from the resonator. This indicates that the quality factor Q increases with increasing WG mode order theoretically. In order to realize high-Q resonances, short wavelength can be employed for excitation.

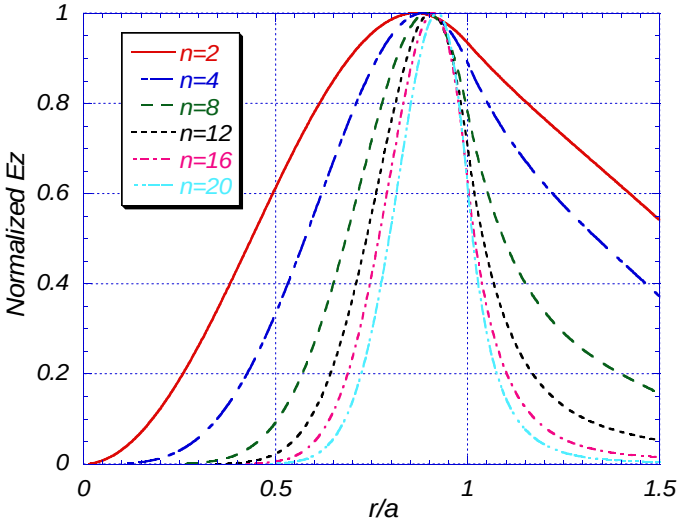

Figure 3. Radial profile of normalized Ez at various modes.

Figure 4 shows the E-field distributions corresponding to (a) 2μm-diameter resonator with $n = 12$ at resonance wavelength of 822.9948nm and (b) 10μm-diameter resonator with $n = 72$ at resonance wavelength of 801.7479nm. Obviously, the 10μm-diameter resonator has better confinement and thus, better mode quality than the small one.

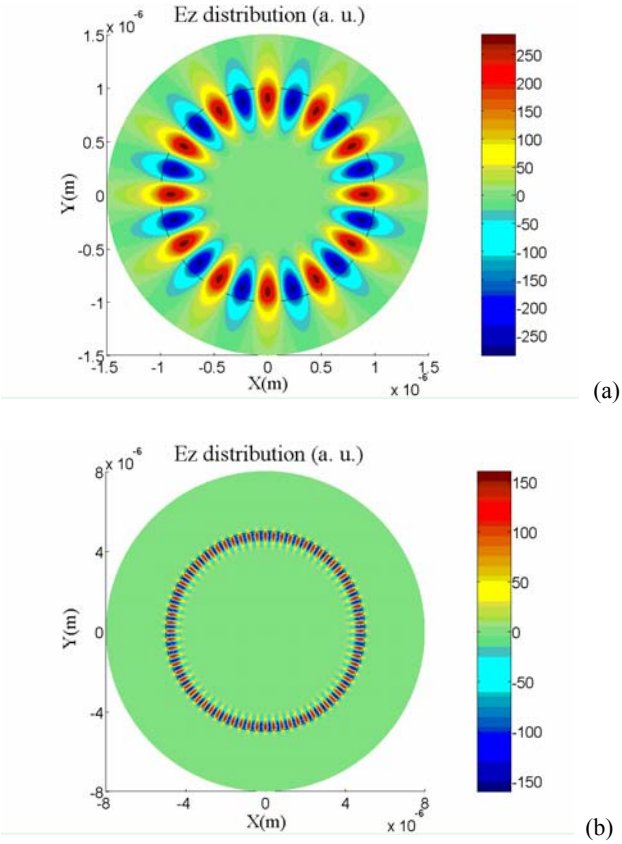

Figure 4. E-field distributions of (a) a 2μm-diameter resonator at (l = 1, n = 12) and (b) a 10μm-diameter resonator at (l = 1, n = 72).

Figures 5 and 6 show the E_z radial profiles and distributions for a 2μm-diameter resonator working, respectively, at WG mode of (l = 1, n = 12) with λ_{ln} = 822.9948nm and at WG mode of (l = 2, n = 12) with λ_{ln} = 656.1893nm. It is observed that there is only one peak in the E_z radial profile for the mode of l = 1, but one peak and one valley for the mode of l = 2.

WG mode resonators can be of any circular geometry (spheres, disks, and rings). Phase-matched optical waveguides or optical fiber cores are used to couple light into the cavity and/or to collect signals. The rapid advances in modern nanofabrication techniques have made it feasible to consider WG mode microcavity resonances in fine and uniform MEMS/NEMS devices having physical dimensions at the micro/nanometer levels. Such devices are manufacturable, and of high uniformity and easy calibration. They usually have a planar structure. Thus, the present study is of importance for intrinsic resonance analysis in MEMS resonators.

CONCLUSION

An analytical method is developed for analyzing whispering-gallery modes in planar structures. The method is based on the solution of the wave equation via the method of

separation of variables. Feasible and appropriate boundary conditions are established for closing the solutions. Analytical formulations are derived. The iteration and bisection methods are utilized for identifying the resonance frequencies/wavelengths. Using this new model, we can easily and precisely find the resonance wavelengths and the E-field peak and valley locations in the radial direction. The calculated results based on the derived formulations are presented for a variety of resonance modes. It is found that the resonance spectrum of a resonator is not uniformly distributed. With increasing azimuthal mode number, more energy will be confined in a very thin layer inside the resonator surface and this will increase the Q. For two resonators working at close resonance frequencies, the large resonator has better mode quality than the small one because the large one has a high resonance mode order.

ACKNOWLEDGMENTS

Z. Guo is grateful to the support of the National Science Foundation (CBET-0541585) to the project.

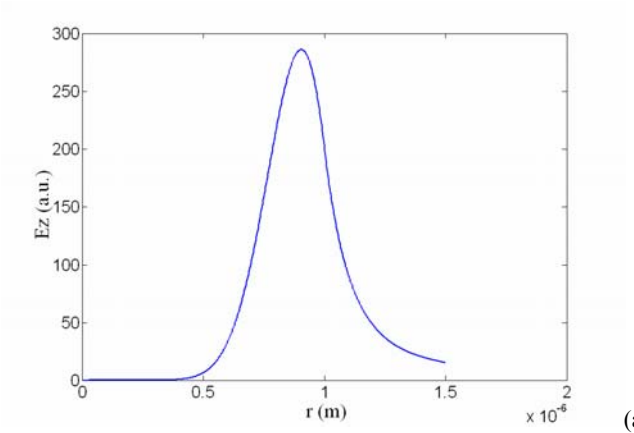

Figure 5. (a) E_Z profile in the radial direction and (b) E-field distributions for a 2μm-diameter resonator at l = 1, n = 12, and λ_n = 822.9948nm.

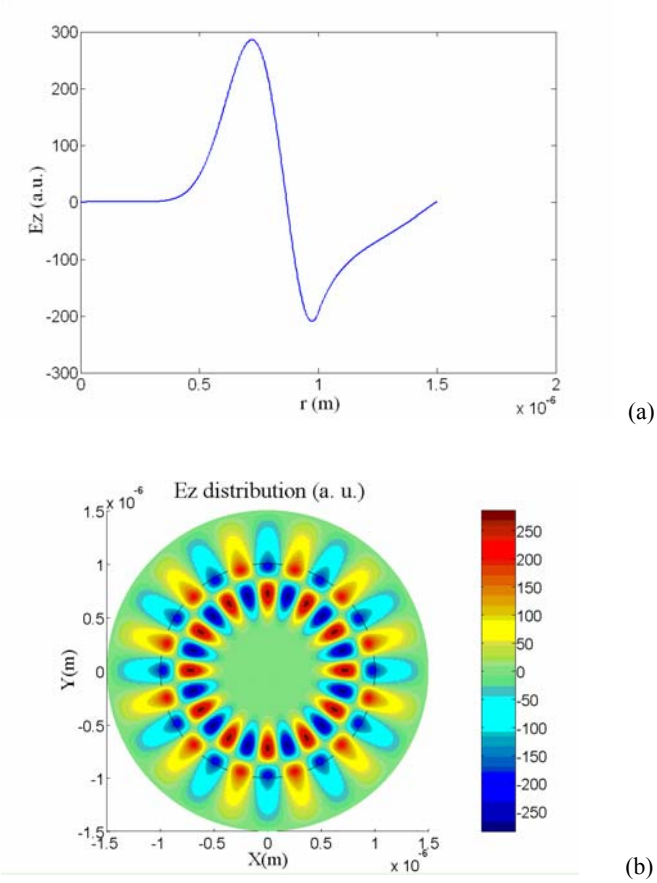

Figure 6. (a) E_Z profile in the radial direction and (b) E-field distribution for a 2μm-diameter resonator at l = 2, n = 12, and λ_n = 656.1893nm.

REFERENCES

[1] Rayleigh, J.W.S., "The problem of the whispering gallery," *Phil. Mag. SG*, **20**, 1001-1004 (1910).

[2] Garrett, C.G.B., Kaiser, W., and Bond, W.L., "Stimulated emission into optical whispering modes of spheres," *Phys. Rev.*, **124**, 1807-1809 (1961).

[3] Braginsky, V.B. and Ilchenko, V.S., "Properties of optical dielectric microresonators," *Sov. Phys. Dokl.*, **32**, p. 36 (1987).

[4] Gorodetsky, M.L., Savchenkov, A.A., and Ilchenko, V.S., "Ultimate Q of optical microsphere resonators," *Opt. Lett.*, **21**, 453-455 (1996).

[5] Vahala, K. J., "Optical Microcavities", *Nature*, 424, 839-846 (2003).

[6] S. Arnold, M. Khoshsima, I. Teraoka, and F. Vollmer, "Shift of whispering-gallery modes in microspheres by protein adsorption," *Opt. Lett.*, **28**, 272-274 (2003).

[7] J.P. Zhang, D.Y. Chu, S.L. Wu, S.T. Ho, W.G. Bi, C.W. Tu, and R.C. Tiberio, "Photonic-wire laser", *Phys. Rev. Lett.*, **75**, 2678-2681 (1995).

[8] E. Krioukov, D.J.W. Klunder, A. Driessen, J. Greve, and C. Otto, "Integrated optical microcavities for enhanced evanescent-wave spectroscopy", *Opt. lett*., **27**, 1504-1506 (2002).
[9] Wasylkiwskyl, W., "Diffraction by a concave perfectly conducting circular cylinder," *IEEE Trans. Anten. And Prog*., **23** (4), 480-492 (1975).
[10] Z. Guo, H. Quan, S. Pau, "Numerical characterization of whispering-gallery mode optical microcavities," *Appl. Opt.*, **45** (4), 611-618 (2006).
[11] Z. Guo, H. Quan, S. Pau, "Near-field gap effects on small microcavity whispering-gallery mode resonators", *J. Phys. D: Appl. Phys.,* **39**, 5133-5136 (2006).
[12] Bohren, C.F. and Huffman, D.R., "*Absorption and scattering of light by small particles*," Wiley-Interscience, New York, 1983.